Title

THE APPLICATION OF HIGH FREQUENCY SEISMIC MONITORING METHODS FOR THE MAPPING OF FLUID INJECTIONS

Author

Majer, E.L.

Publication Date

1987-04-01

Lawrence Berkeley Laboratory
UNIVERSITY OF CALIFORNIA

EARTH SCIENCES DIVISION

Presented at the Workshop on Forced Fluid Flow through Fractured Rock, Paris, France, April 13–16, 1987

The Application of High Frequency Seismic Monitoring Methods for the Mapping of Fluid Injections

E.L. Majer

April 1987

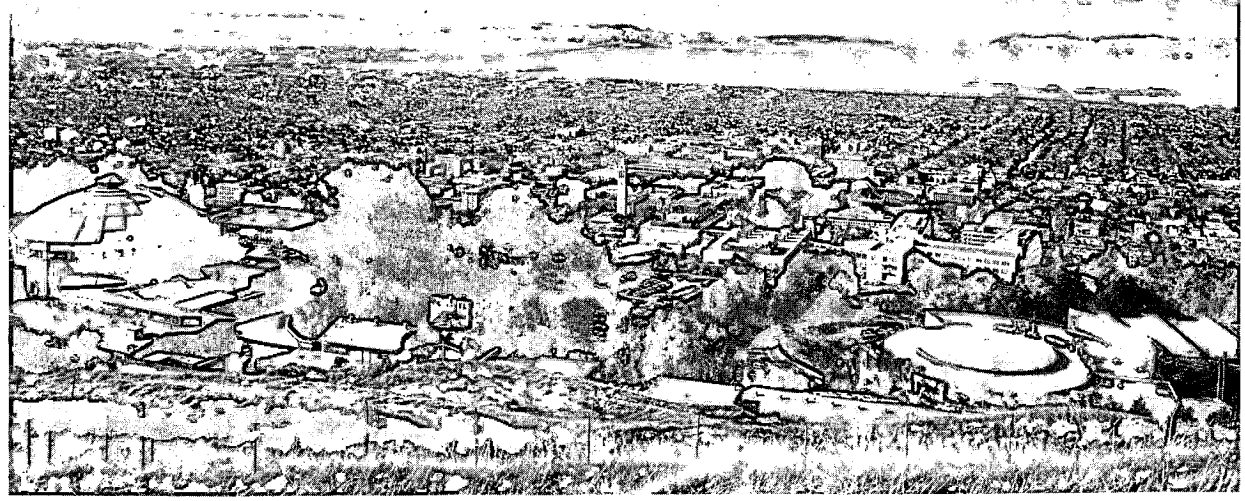

Prepared for the U.S. Department of Energy under Contract DE-AC03-76SF00098

DISCLAIMER

The Application of High Frequency Seismic Monitoring Methods for the Mapping of Fluid Injections.

E.L. Majer

Center for Computational Seismology, Lawrence Berkeley Laboratory,
Earth Sciences Division,
University of California, Berkeley, California 94720

INTRODUCTION

This paper describes the experimental work we have been carrying out using seismic methods for monitoring the path of fluid injections. The most obvious application is the high pressure fluid injections for the purpose of hydrofracturing. Other applications are the injection of grout into shallow subsurface structures and the disposal of fluids in the geothermal and toxic waste industries. In this paper hydrofracture monitoring and grout injections will be discussed.

To date, in terms of field monitoring, the seismic techniques are the most advanced. Also, there is already a significant number of case histories using seismic monitoring to determine fracture properties (Power et. al., 1976). There has been some monitoring using electrical techniques, primarily magnetic, but it is not as extensively used as the seismic techniques.

For years earthquake seismologists have been concerned with characterizing the seismic signals generated from a fracture embedded in a medium. The goal of these studies has been to specify the dynamic source properties: fracture orientation, dimensions, time history and stress distribution from the seismic waveforms. No assumptions are made beforehand on the orientation or type of source. In the case of an earthquake, the propagating "fracture" is a fault. In the case of a hydrofracture each "jump" of the total fracture length could be considered as a small earthquake. The frequency content and amplitude of the seismic signals given off by a fracture depend upon its dimensions, nature and rate of stress release, amount of displacement, and the rock properties. Stated in another way, given the variation of ground displacement (radiation pattern) produced by a seismic source, and a reasonable estimate of the propagation effects, then the source of the seismic disturbance can be located and separated into components such as shear, tension, etc. We know from lab and small scale field experiments that seismic signals are generated during and after the hydrofracture process (Majer et. al., 1983). It appears sensible to use these first order effects to track the fluid path, and to apply the techniques for source property determination developed for earthquake seismology.

Using seismic methods for hydrofracture characterization or grout monitoring is not a new idea. Because the seismic signals that radiate from fracturing are a first order

effect, it seemed reasonable to others to monitor these signals (Pearson, 1981). Also, because of the relative high frequency nature of the signals as compared to tilt or magnetic measurements, the seismic methods potentially offer a real-time method with greater resolution for monitoring. Most efforts in the past have been to place single sensors either on the surface or in a nearby well to detect the P- and/or S-waves created from the fracturing. In some instances sensors were placed at the top of the well or on the casing. The results of these experiments were mixed at best. Such factors as improper sensors (inadequate bandwidth or wrong natural frequency), large amounts of noise from pumping operations and/or severely attenuated signals, caused most to abandon this technique. There have, however, been more sophisticated seismic techniques attempted (Smith et al., 1978; Nyland and Dusseault, 1983). Power et al. (1976) described an experiment where a large array of instruments was placed around a well that was being fractured. The results were quite encouraging, considering the depth of fracture, 9000 feet. Such features as fracture azimuth, length, and degree of symmetry were inferred.

The purpose of the subject seismic field experiments is to map the hydrofracture/grout geometry in detail using a 3-D array of seismic sensors surrounding the injection zone. Seismic methods potentially offer the most direct approach to mapping fluid geometry. During the past several years we have carried out various laboratory and field experiments to determine the applicability of seismic techniques to trace the path of a hydrofractureand grout injections. Laboratory and small scale field experiments have shown that the "fracture" is really a sum of smaller discrete fractures, occurring over the total length of the hydrofracture path (Solberg et al., 1977; Majer et al., 1983; Majer et al., 1984). The dominant failure mechanism observed in these laboratory experiments has been tensile failure, however, if in-situ stress conditions are favorable, shear failure has also been observed.

Ideally, from a monitoring point of view, what is sought is a seismic discriminant that would determine the mechanisms which are generating the seismic waves. Depending on the partitioning of energy from the fluid injection process, and how much of this energy is spent in breaking the rock and how much energy is being absorbed in the fluid, the rate and manner of the energy release will be reflected in the type of seismic waves generated. Such factors as rock strength, permeability, porosity, pressure gradients, fluid compressibility, and volume will all affect the rate and manner of energy release in the form of seismic activity. How these factors all interact during the fluid injection, and to what extent they are reflected in the seismic activity as well as the pressure transients is the subject of the seismic study.

As with any geophysical method, the farther away from the source of the anomaly, the more difficult it is to collect sufficient data for accurate interpretation. Such factors as noise and attenuation degrade the data and make detailed estimates of the desired properties more difficult. In the use of seismic methods, the desired signals are the elastic waves generated during the hydrofracturing process. There will be many different sources of these seismic waves during the operation. However, each different source of seismic waves has its own unique mechanism of generating these signals. Because of this, the signals associated with each source have coded in them the mechanisms that created it. At any particular point in space and time during the hydrofracture process one can monitor the ground motion, i.e., the seismic waves as they disturb the media that they are propagating in. Depending on the shape, orientation, magnitude and proximity of

the source, the signals will have varying frequency content and amplitude.

Assuming passive monitoring of the fluid injection, there are two basic approaches detecting the seismic signals. The first and most straightforward is monitoring the discrete events associated with the process. This is essentially monitoring and processing the acoustic emission events as if they were earthquake events. The second approach is to treat the fluid sheet or volume as a continuous generator of seismic energy (such as the reflected seismic energy from a vibrator source used in seismic reflection surveys) and utilize imaging techniques to trace the growth of the fluid volume as the signals change due to variations in the injected fluid volume. It has also been proposed that the "crack" flexes with pressure variations in the pumping sequence. If it "flexes" enough it may produce a signal that could be detected by "stacking" the signals. As the length of the fracture changes, the characteristic frequency of the signal emitted will also change thus giving an indication of fracture length. With a properly designed array, azimuth may also be inferred.

HYDROFRACTURE MONITORING

Hydraulic fracturing was first used in 1949 for stimulating unproductive oil wells (Krueger, 1973). The first theoretical study was by Hubbert and Willis (1957) which pointed out the tensile nature of the fractures at the borehole wall. Additional theoretical studies were carried out by Scheidegger (1962), Kehle (1964) and Fairhurst (1964). Haimson and others (1968, 1969, 1970, 1972) in a series of papers pointed out the role of fluid penetration, pore pressure and the applicability of the technique for monitoring stress in deep environments. Laboratory experiments by Lockner and Byerlee (1977) have also characterized the fracture process in terms of tensile and shear failure depending on the differential stress, rock permeability, viscosity and injection rate of the fracturing fluid. In triaxially stressed specimens, Solberg et al. (1977) found that shear failure could play just as an important role in the fracturing process as tensile failure. In addition to laboratory studies, numerous computer programs have been written to model the hydraulic fracturing process (Cleary, 1979, 1983; Daneshy, 1973; Palen and Narasimhan, 1981). The aim of most of these model studies has been to understand the pressure-transient records that are derived during hydraulic fracturing. The models are complex enough to include wellbore storage, fracture storage, fracture damage in the form of a fracture skin or restricted fracture flow capacity, asymmetric fracture geometry, and deformable proppant-fracture systems.

One of the first field experiments we carried out to characterize a hydrofracture in detail using seismic techniques was performed in granite at Stripa, Sweden (Majer and McEvilly, 1982). Prior to this it was not known if shear or tensile failure could be observed and characterized using conventional seismic instrumentation and analysis techniques. This experiment clearly demonstrated that discrete events were occurring, and these events could be treated as individual "nanoquakes" to trace the growth of the fracturing. The principal mechanism of failure observed at Stripa was shearing. Pearson (1981), from monitoring hydrofractures in granite, also concluded that the events most likely to be detected at distances up to thousands of feet during hydrofracture operations were shear failures induced by pore pressure increases. Batchelor (1982), in a similar experiment in granite, also reported seeing shear failure during the pumping

phases of a water hydrofracture operation in a "hot dry rock" environment. However, no signals were detected at large distances away from the fractured zone (several thousand feet) when the fracturing fluid was a gel. The shear events detected in all of these cases were probably in response to fluid filling the fractures in the immediate vicinity of the fluid path, causing failure when the fluid pressure (pore pressure) reduced the confining pressure to allow failure or slip consistent with the maximum principal stress directions.

In a more recent laboratory experiment (Majer et al., 1983), five acoustic emission (AE) sensors were placed on the side of a 12" by 12" by 18" salt cube under a triaxial load (2000 $\times$ 2000 $\times$ 3000 psi). The cube was then hydrofractured using oil as the fluid. To our knowledge this was one of the few laboratory experiments where a hydrofracture of this scale was monitored with sufficient detail to watch the fracture mechanisms as the fracture grew. Although the duration of pumping was only thirty seconds in length, several thousand discrete events were recorded and analyzed. Each event was located, the P- and S-waves windowed, and FFT's performed on these windowed data. With these spectral data, source parameters were inferred and related to the stress information. The significant results were:

(1) The hydrofracture process is a series of discrete events, whose sum makes up a network of fractures into one large fracture. The path of the fracture mapped with seismic methods corresponded almost exactly to the actual path that was shown by using a dyed oil.

(2) There was no evidence of shear failure in salt. It must be kept in mind that there was no pore pressure in these experiments, all samples were dry, and the confining pressures were applied with a flatjack loading system.

(3) There was a definite correlation between pumping rate and AE activity.

(4) The larger events, both in stress drop and in energy release, were near the borehole, where higher stress concentrations occurred.

(5) The source size seemed to be governed by inhomogeneities, i.e., there were no events larger than the average grain size.

(6) The overall direction of the fracture was determined by direction of the least principle stress (perpendicular), although the detailed path was determined by inhomogeneities (grain boundaries) in the rock.

The time history of event occurrences is shown in Figure 1. These findings implied that if one could get close enough to the process (we were 20 to 30 times the source dimension of each seismic event away) then details of the fracture growth could be unraveled. What was lacking, however, in this experiment was pore pressure, and a realistic rock type.

At a slightly larger scale, a series of hydrofractures were monitored at a depth of 200 ft in granite. The layout of the experiment is shown in Figure 2. The experiment was carried out at the bottom of a Canadian mine that is being excavated for research in nuclear waste storage. Four holes were drilled, three observation and one hydrofracture. Emplaced in each of the observation holes were four piezoelectric accelerometers, forming a 12-element 3-D array of seismic sensors. The data were amplified with broad band amplifiers (500 to 200,000 Hz) and recorded on a Honeywell 5600 C tape recorder (300 to 300,000 Hz). Shown in Figure 3 are examples of the events recorded. Events 1 and 2

were the most typical, impulsive, with clearly defined P waves. These are due to tensile failure of the rock. We also observed events with P and S waves, indicating a certain amount of shear failure. However, also observed was seismic activity of the type shown in events 3 and 4 of Figure 3. These were emergent type events with durations often 5 to 10 times as long as the impulsive events. These are possibly in response to the resonance of the fluid rock system, thus creating "harmonic tremor" type events. If one plots the location of the events then the path of the hydrofracture is mapped in detail, as shown in Figure 4. Overcoring and seismic results almost exactly agree as to the location of the hydrofracture. However, impression packer work indicates, at least at the borehole wall, that the fracture was oriented 20% from the path defined by the seismic results. Again we had confirmation that the hydrofracture process can be mapped by locating the discrete seismic activity.

GROUT MONITORING RESULTS

Figure 5 is the layout of the field experiment. The grout monitoring experiments were carried out at an U.S. Army Corps of Engineers site in Oregon on the Columbia River. The rock type was the Columbia River basalts. The permeability of the fractured rock mass varied from .000001 to .0000001 M/sec. The work was funded by the Army corps of engineers as part of a larger progect to determine and refine proper grouting practices in fractured rock. As can bee seen, the objective of the experimental setup was to use a 3-D array of sensors to monitor the seismic signals generated during the grouting operations. The approach was to use a wide band monitoring array, both in space and time, to characterize the nature of the seismic signals from the fluid movement and/or rock movement. Varied was the viscosity, flow rate and pressure. The actual field values used are shown in Figures 6, 7, 8, and 9. In the SS holes in Figure 5 were Wilcoxin 417T transducers grouted in place at approximately 30 feet below the surface. The frequency response of these transducers is from 2.0 hz to 9,000 hz (3db point), with a mounted resonance of 16,000 hz. the sensitivity of the 417T is 4.5 volts/g at 100 hz. In the HF holes were Columbia 5005 transducers with a frequency response of 2.0 hz to 10,000 hz with a resonance of 50,000 hz. The sensitivity of the Columbia instruments is .015 volts/g. As one might guess the Columbia transducers are much better above 20,000 hz where the Wilcoxin are better below 20,000 hz. The A/O holes were for the emplacement of linear arrays of the Wilcoxin transducers. In each array there were five transducers mounted 18 inches apart. There were two field experiments in this project. In the first experiment one array was suspended in a water filled hole. This did not provide adequate coupling to the rock. For the second experiment we built a second array and have put a packer system on the both arrays to provide better coupling to the formation.

The sequence of the experiment was to essentially create a fracture system by overpressurizing the rock. The next step was to inject water, thin, medium, and thick grout into this fracture system and monitor the seismic signals with the instruments mentioned above. The data were recorded on a 14 channel analog direct-record tape recorder. Its band width is from 100 hz to 75,000 hz. Also recorded was a signal used for timing purposes, a 10,000 hz sawtooth, and the well head pressure. The pressure was recorded by using a Sensotek 0-5,000 psi foil gauge pressure transducer. The resolution

of the pressure transducer was about 1 PSIA. The frequency response of the pressure transducer was from dc to 5,000 hz. Because we passed the pressure signal through a VCO in order to record the pressure signal on a direct record tape recorder, this limited the frequency response of the pressure signal to no more than 100 hz. However, through the combination of all the different sensors we were able to monitor the signals from dc to 75,000 hz.

As mentioned above there exists a possibility for two different types of events, and combinations in between, discrete acoustic emission (AE) events with clearly defined P- and/or S-waves and continuous noise at some characteristic frequency that depends upon the source characteristics. What was recorded was both types of signals and combinations of these signals. There were occurrences of discrete AE signals in all injections, but the occurrence rate of these discrete events varied significantly, as can be seen in Figures 6, 7, 8, and 9. Shown in these figures is the rate of AE, pumping rate, and flow rate as a function of time. The AE activity is an integrated energy shown for individual channels. The channels shown is activity detected in three of the the SS holes. Only three of the SS holes detected significant activity, with the fourth hole showing little or no activity. As discussed later this was due to the pattern of grout flow. The general trend, except for water, was that there was a decrease in AE activity as the viscosity of the fluid increased. Although in each case AE activity increased as the flow rate and pressure increased. It also appears that the seismic energy is released in larger but fewer events as the viscosity increases. However, as the viscosity increases the background noise or continuous signal also increases as a function of flow rate. In a typical grout operation these continuous signals will be the most abundant signals. There was also a lack of any increase in background or continuous signal level in the water injection. However, there was a considerable signal level increase at higher pressures with the thick grout at higher flow rates.

At the higher viscosities we could not get the higher flow rates due to the tightness of the rock. It does appear from the tests to date that the lower threshold of detection at the scales of a few 10's of meters is on the order of 0.5 to 1 gal/minute. Another significant finding is the frequency content of the signals. The pump noise and noise to to surface activities is in the range 10 to 100 hz. The discrete signals are from 5,000 hz to 20,000 hz, with the majority in the range of 5,000 to 10,000 hz. The continuous signals are mainly from 1,000 hz to 5,000 hz. Therefore, as we suspected, the pump noise and surface activities are not a problem. In all the data processed to date no filtering, has been done, it is as it was recorded. Some data have been filtered with a high pass butterworth filter at 3,000 hz to determine the signal to noise improvement. There is approximately a 6 to 12 db improvement in signal to noise ratio after filtering the data. In the future field experiments the amplifiers will have been modified to put a high pass filter at 1,000 hz and their gain raised by a factor of 4 to 400. Including the gain in the transducer preamp we now have a gain of 4,000 on our array of transducers. That is, our sensitivity is 1800 volt/g from 1,000 hz to 16,000 hz. Our noise floor on our tape recorder in this bandwidth is about 10 millivolts. Therefore, our detection threshold will be about 5 to 10 micro-g's between 1,000 hz and 16,000 hz.

Shown in Figures 10 and 11 are the approximate boundaries of the grout. The contours are the edges of the extent of the AE events. The four different contours are 25, 50, 75 and 100 percent of the events. Notice that the grout sheet grew differently than the water. This suggests that as the viscosity changes the fluid will take different paths,

even though all else is the same. It is hoped that in the case of normal grouting operations the extent of the grout will be determined by a combination of locating the AE events and by properly processing the the continuous signals as a function of amplitude and frequency content. Two approaches will be tried with the data collected from the linear arrays, frequency-wavenumber and beamforming. One might also consider wavefield migration, but it may not be necessary.

At this point in the project we have clearly demonstrated the viability of using seismic signals in the range of 1,000 to 20,000 hz for the real time mapping of grout injections. Up to this time we have been using Poly-sal as a grout simulator. Some may object that this may not be representative of a true grout. If anything, I would expect normal grout to act more favorably relative to the generation of seismic signals. Poly-sal has no abrasives as does a grout. This will make the fluid more resistant to flow at the same pressure in the same fracture. Therefore, the fluid flow will not be as continuous and it will impart more seismic energy to the rock in a grout job versus a Poly-sal job.

As far as designing a field system to implement in a real situation it must have the following features: (1) variable gain amplifiers on the input channels, (2) variable bandwidth filter settings, (3) digital sampling at 12-bit resolution at up to 100,000 samples/sec, (4) 16 input channels, (5) one MIPS processing capability. One candidate is: a Transient Waveform Analyzer/PC/Array Processor system. The cost of this system would be about 30,000 USD. At the present time we are building such a system to be used for routine grout monitoring. With proper signal conditioning it is quite possible to detect and record the signals necessary for mapping grout sheets in real time. The question now is how far can we push the method to apply to as many different rock environments as possible.

SUMMARY

In large scale monitoring projects we have encountered phenomena that can not be observed in laboratory experiments due to lack of realistic conditions, nor are predicted or explained from models or theoretical studies. To understand and refine the hydrofracture method, as well as develop monitoring techniques for grout and other fluid injections, controlled experiments in a reduced but realistic situation must be carried out. Combined with these field measurements the modeling will aid in determining the proper monitoring techniques for mapping the fluid path geometry and unravel the mysteries of this complicated fluid-rock system.

We know from experiments to date that by using discrete seismic events we are definitely capable of tracking the fracture in detail and discriminating between the various failure mechanisms. The problem, however, has been that no one has monitored hydraulic fracturing in sufficient detail, or simultaneously related the detailed near field information to the far field geophysical and pressure data. If we are to understand the phenomena observed, and relate them to the fluid injection process, we must carry out a controlled seismic experiments at reasonable scales. The technique if properly applied can be a great aid in understanding not only the geometry of the hydrofracture and/or grout path, but more importantly how it developed.

ACKNOWLEDGMENTS

This research was supported by the U.S. Army Corps of Engineers Waterways Research Station, and by the director, office of Basic Energy sciences, Division of Engineering, Mathematics, and Geosciences, and the office of Civilian Waste Management of the U.S. Department of Energy under contract DE-AC03-76SF00098.

Figure Captions

Figure 1. Plan view of discrete event locations during a laboratory hydrofracture of a salt block. Panel 1 is 25% of the event, Panel 2 is 50%, Panel 3, 75% and Panel 4, 100% of the events located. Total time = 30 sec.

Figure 2. Experimental set-up to monitor the discrete seismic activity at the Canadian site.

Figure 3. Example of waveforms recorded at the Canadian site, 95% were of type 1 and 2.

Figure 4. Plan view of location of discrete events in the Canadian experiment.

Figure 5. Experimental set-up for the grout monitoring experiments. The SS holes were the locations of grouted in single sensors with a band width up to 8,000 hz. The HF holes contained higher frequency sensors. The A/O holes were used to visually monitor the grout path and to locate moveable arrays of AE sensors.

Figure 6. The AE activity in three of the SS holes, the pressure, and flow rate as a function of time for a water injection. The viscosity (27 sec) is a marsh funnel viscosity.

Figure 7. The AE activity in three of the SS holes, the pressure, and flow rate as a function of time for a thin grout injection. The viscosity (32 sec) is a marsh funnel viscosity.

Figure 8. The AE activity in three of the SS holes, the pressure, and flow rate as a function of time for a medium grout injection. The viscosity (47 sec) is a marsh funnel viscosity.

Figure 9. The AE activity in three of the SS holes, the pressure, and flow rate as a function of time for a thick injection. The viscosity (59.4 sec) is a marsh funnel viscosity.

Figure 10. The approximate location of the water front as a function of AE activity. The contours show the integrated energy release in increments of 25 percent.

Figure 11 Same as Figure 10 but for the medium grout injection. Notice that the grout did not travel in the same location as the water.

References

Batchelor, A.S., 1982, The stimulation of a hot dry rock reservoir in the Cornubian Granite, England: *Proc. of the 8th Workshop on Geothermal Reservoir Engineering, Stanford University.*

Cleary, M.P., 1979, Rate and structure sensitivity in hydraulic fracturing of fluid-saturated porous formations: *Presented at the 20th U.S. Symposium on Rock Mechanics, Austin, Texas, June 4-6.*

Cleary, M.P., 1983, Modelling and development of hydraulic fracturing technology: *In* Rock Fracture Mechanics, Springer-Verlag, (H.P. Rossmanith ed.) 383-476.

Cornet, F.H. and Valette, B., 1984, In-situ stress determination from hydraulic injection test data: *J. Geophys. Res. 89,* 11527-11538.

Daneshy, A.A., 1973, A study of inclined hydraulic fractures: *Soc. Pet. Eng. J.,* April, 61-68.

Haimson, B.C., 1968, Hydraulic fracturing in porous and nonporous rock and its potential for determining in-situ stresses at great depth: Ph.D. Thesis, University of Minnesota.

Haimson, B.C. and Fairhurst, C., 1969, Hydraulic fracturing in porous-permeable materials: *AIME Petrol. Trans.,* 811-817.

Haimson, B.C. and Fairhurst, C., 1970, In-situ stress determination at great depth by means of hydraulic fracturing: *In* Rock Mech.--Theory and Practice, Proc. of 11th Symposium on Rock Mechanics (ed. Somerton, Soc. Mining Engineers of AIME), 559-584.

Haimson, B.C. and Stahl, E.J., 1970, Hydraulic fracturing and the extraction of minerals through wells: *In* 3rd Symposium on Salt, Northern Ohio Geol. Soc., Cleveland, Ohio, 421-432.

Haimson, B.C. and Edl, J.N., Jr., 1972, Hydraulic fracturing of deep wells: *AIME, Petrol. Trans. 4061,* 1-12.

Hubbert, M.K. and Willis, D.G., 1957, Mechanics of hydraulic fracturing: *Trans. AIME 210,* 153-163.

Kehle, R.O., 1964, Determination of tectonic stresses through analysis of hydraulic well fracturing: *J. Geophys. Res. 69,* 259.

Krueger, R.F., 1973, Advances in well completion and stimulation during JPT's first quarter century: *J. Pet. Tech.,* December, 1447-1462.

Lockner, D. and Byerlee, J., 1977, Hydrofracture in Weber sandstone at high confining pressure and differential stress: *J. Geophys. Res.*

Majer, E.L., Mauk, F.J., and Sorrells, G.G., 1984, Utilizing seismological techniques for

monitoring hydrofracture geometry: *EOS.*

Majer, E.L. and McEvilly, T.V., 1982, The Stripa acoustic emission experiment: *Proc. of the Workshop on Hydraulic Fracturing for Stress Measurements. U.S.G.S. Open File Report 82-1075,* 569-582.

Majer, E.L. and McEvilly, T.V., 1984, Acoustic emissions and wave propagation monitoring at the Spent Fuel Test-Climax: *Int. J. Rock Mech. & Min. Sci.* v. 22, No. 4, pp 215-226.

Majer, E.L., McEvilly, T.V., and Doe, T.W., 1983, Laboratory studies of acoustic emissions (AE) in salt during hydrofracturing: *EOS 64,* (45).

Nyland, E. and Dusseault, M., 1983, Fire flood microseismic monitoring results and potential for process control: *J. Canadian Petrol. Tech.,* March-April, 61-68.

Palen, W.A. and Narasimhan, T.N., 1981, The roles of pore pressure and fluid flow in the hydraulic fracture process: Ph.D. Thesis, University of California, Berkeley. Lawrence Berkeley Laboratory report LBL-13049.

Pearson, C., 1981, The relationship between microseismicity and high pore pressures during hydraulic stimulation experiments in low permeability granite rocks: *J. Geophys. Res. 86,* (B9), 7855-7865.

Power, D.V., Shuster, C.L., Hay, R., and Twombly, J., 1976, Detection of hydraulic fracture orientation and dimensions in cased wells: *J. Petrol. Tech.,* 1116-1124.

Scheiegger, A.E., 1962, Stresses in the earth's crust as determined from hydraulic fracturing data: *Geologie und Bauwesen 7,* 45-53.

Smith, M.B., Holman, G.B., Fast, C.R., and Covlin, R.J., 1978, The azimuth of deep, penetrating fractures in the Wattenberg field: *J. Petrol. Tech.,* 185-193.

Solberg, P., Lockner, D., and Byerlee, J., 1977, Shear and tension hydraulic fractures in low permeability rocks: *Pageoph. 115,* 191-198.

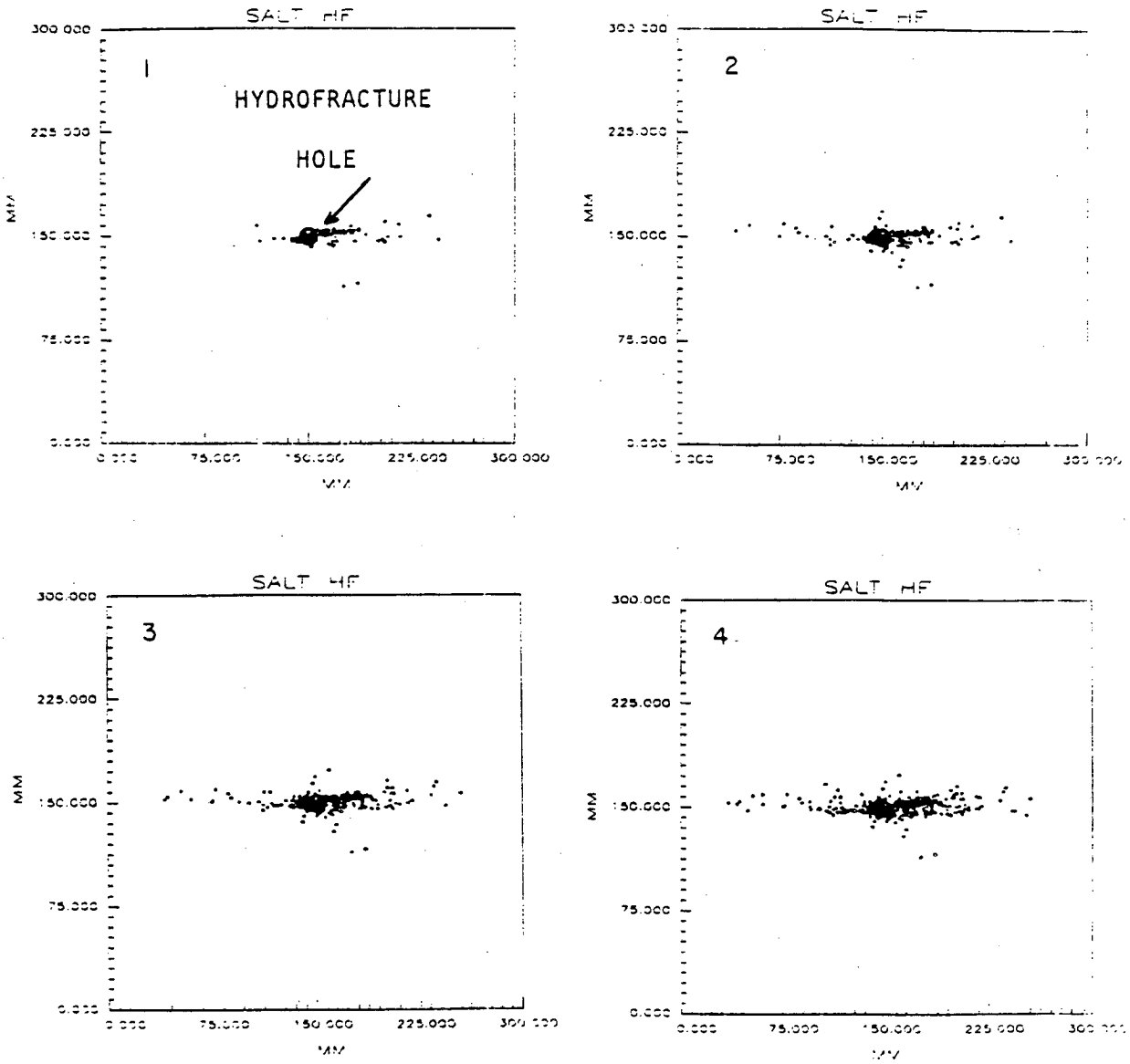

PLAN VIEW

E

N S

W

FIGURE 1

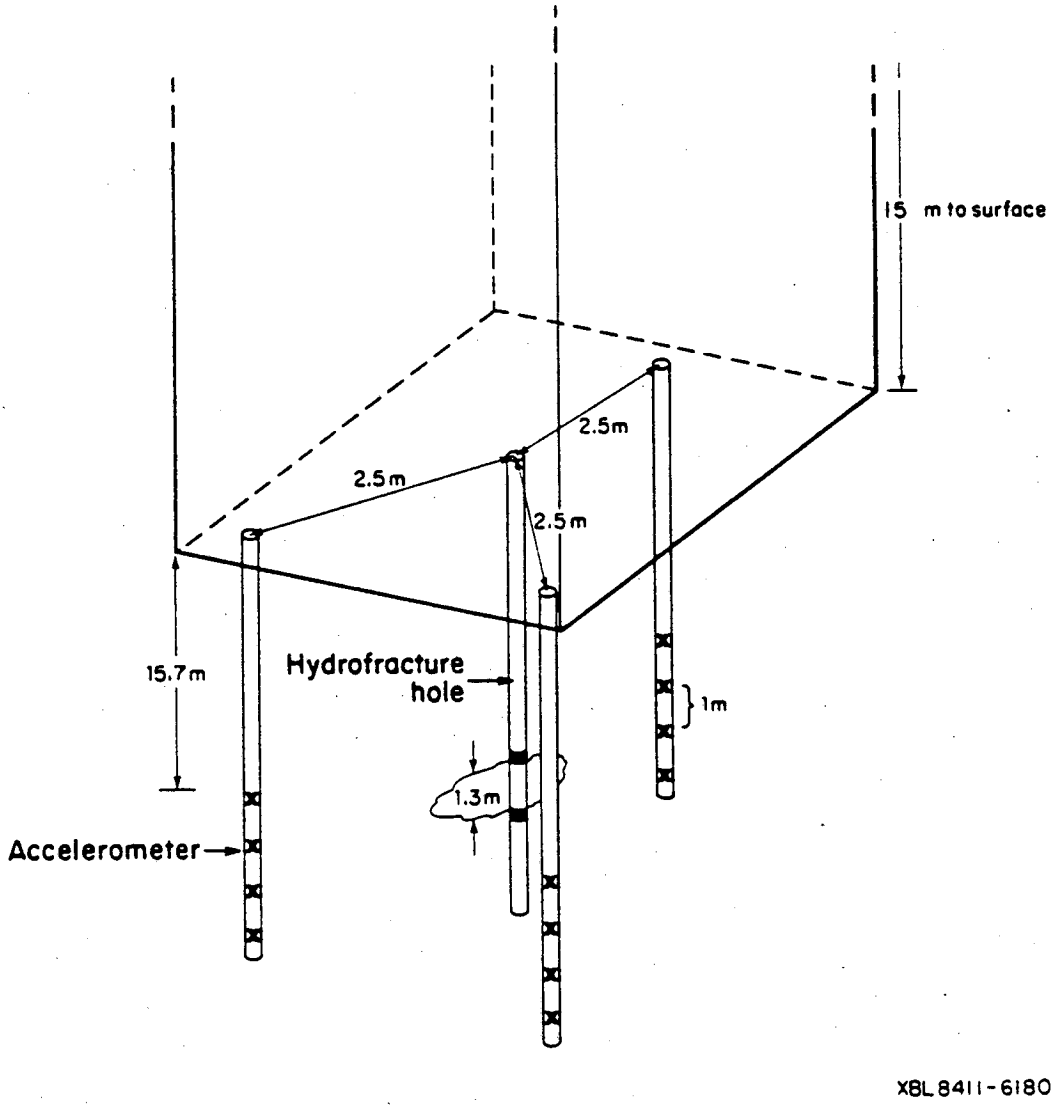
Canadian Mine-Back Experiment
15 m to surface
2.5m
2.5m
2.5m
15.7m
Hydrofracture hole
1m
1.3m
Accelerometer
XBL 8411-6180

FIGURE 2

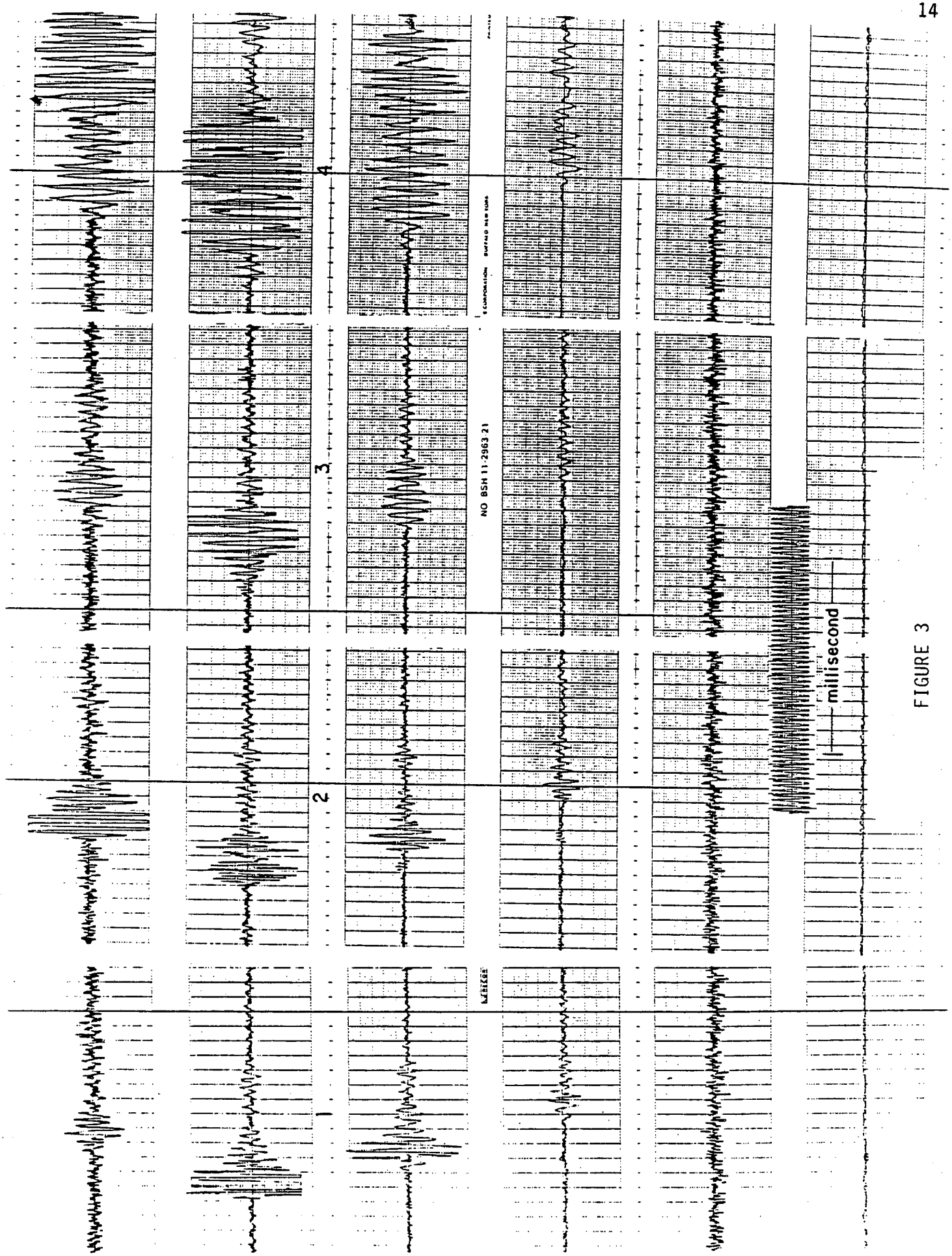

FIGURE 3

PLAN VIEW

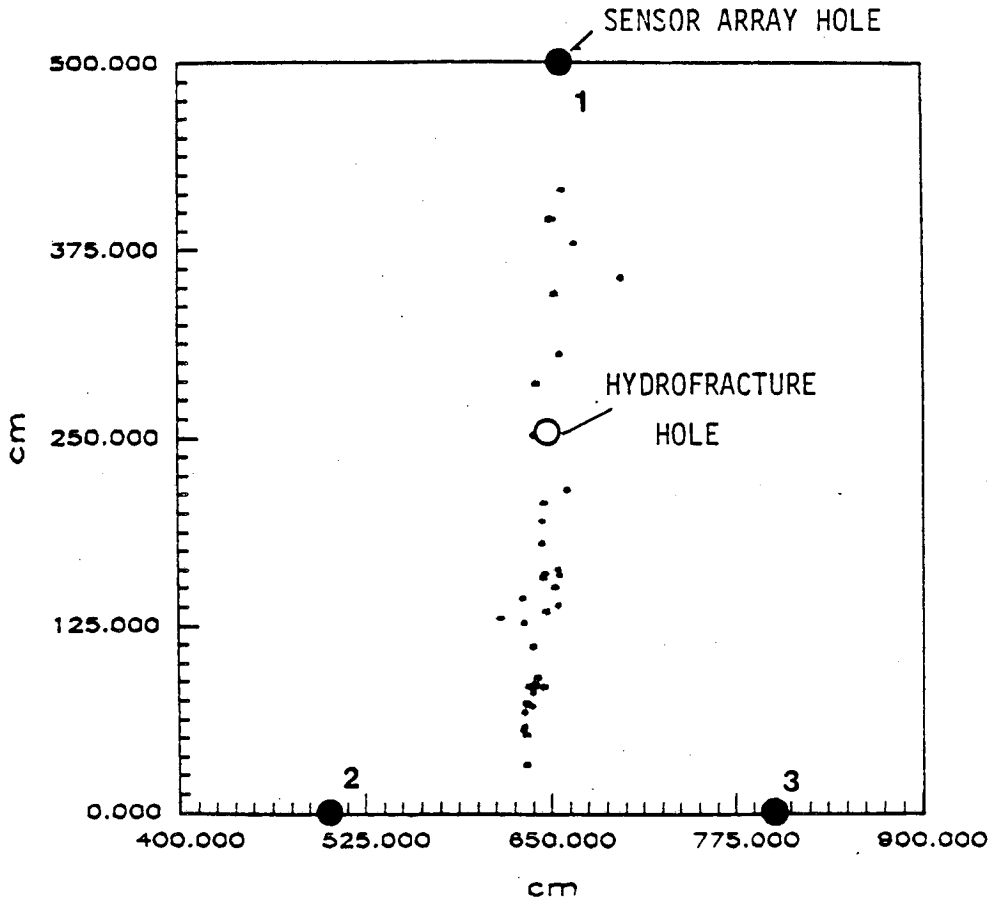

XBL 8412-5216

FIGURE 4

Grout Injection Experiment
McNary Dam, Umatilla, Oregon

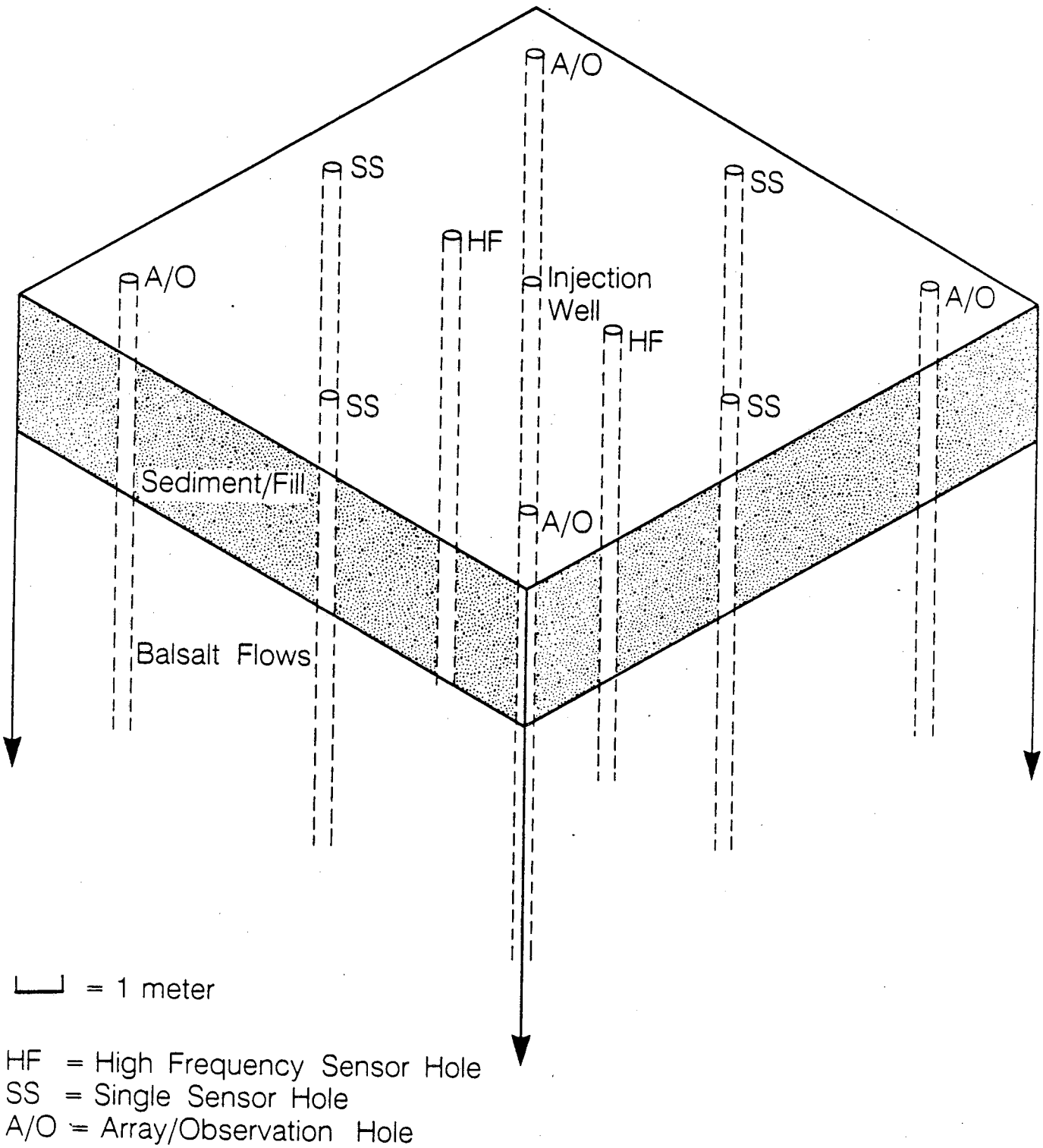

XBL 868-10957

FIGURE 5

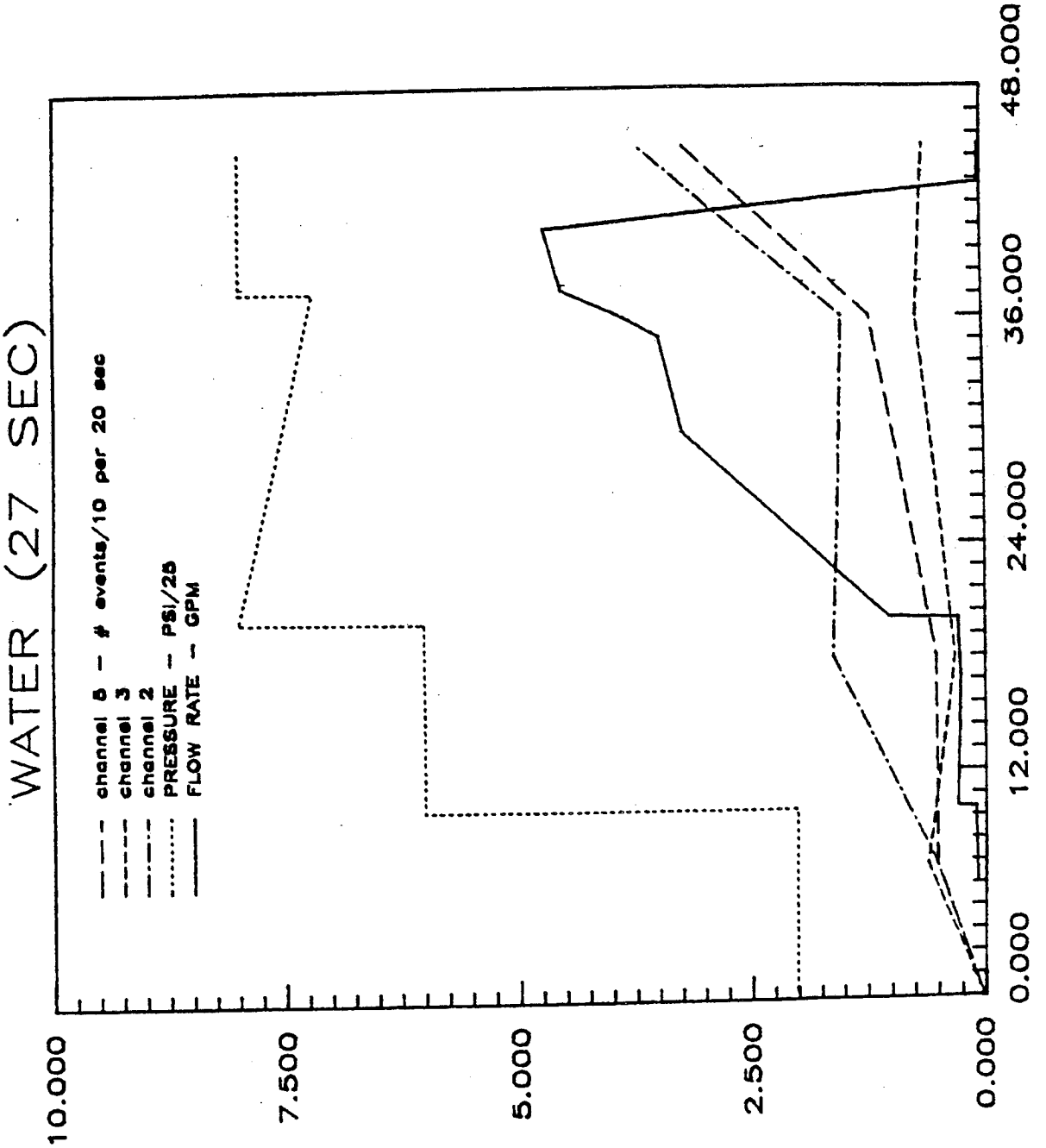
WATER (27 SEC)
channel 5 - # events/10 per 20 sec
channel 3
channel 2
PRESSURE -- PSI/25
FLOW RATE -- GPM
10.000
7.500
5.000
2.500
0.000
0.000
12.000
24.000
36.000
48.000
TIME (MIN)

FIGURE 6

FIGURE 7

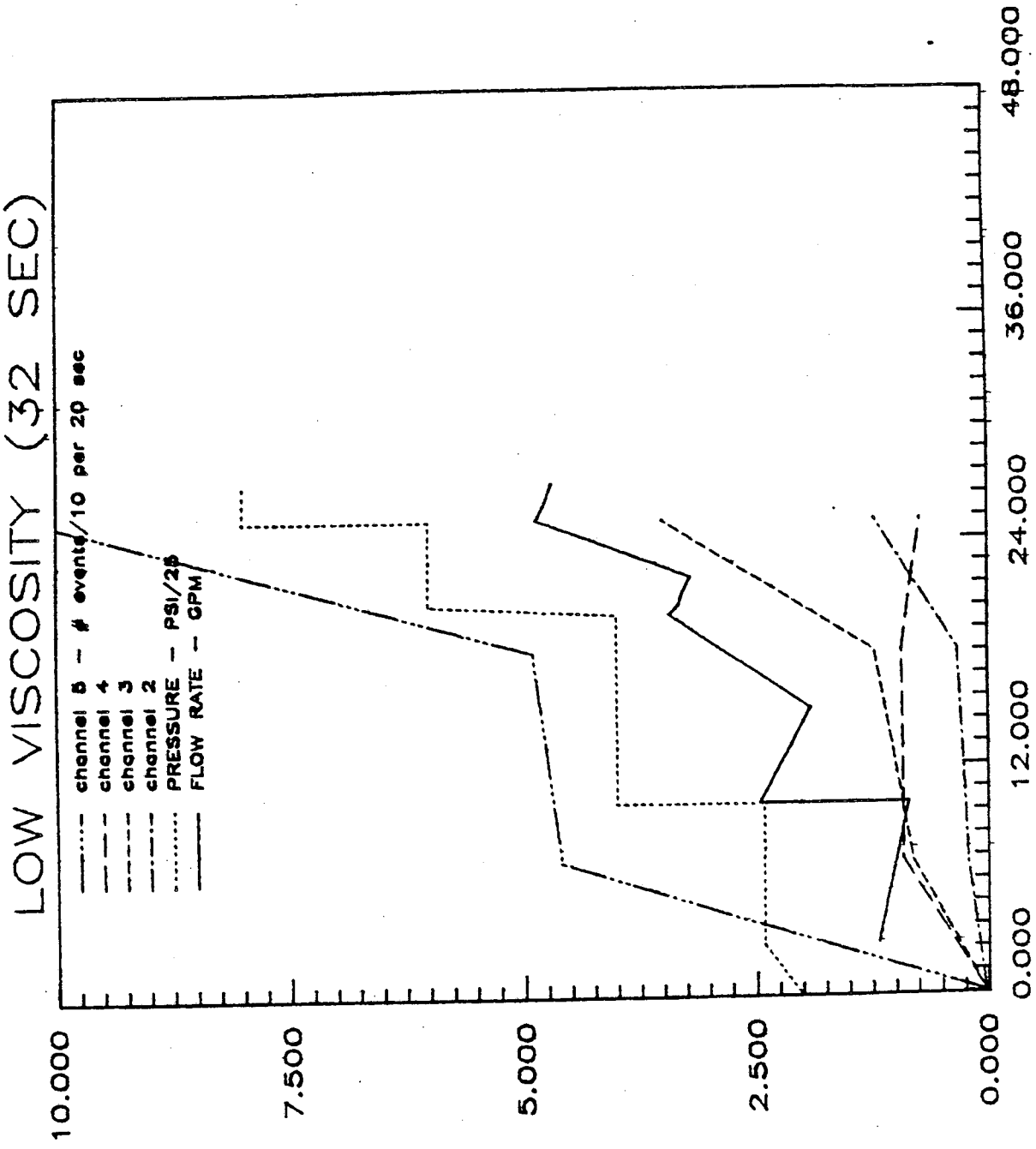
LOW VISCOSITY (32 SEC)
channel 5 - # events/10 per 20 sec
channel 4
channel 3
channel 2
PRESSURE - PSI/25
FLOW RATE - GPM
10.000
7.500
5.000
2.500
0.000
0.000
12.000
24.000
36.000
48.000
TIME (MIN)

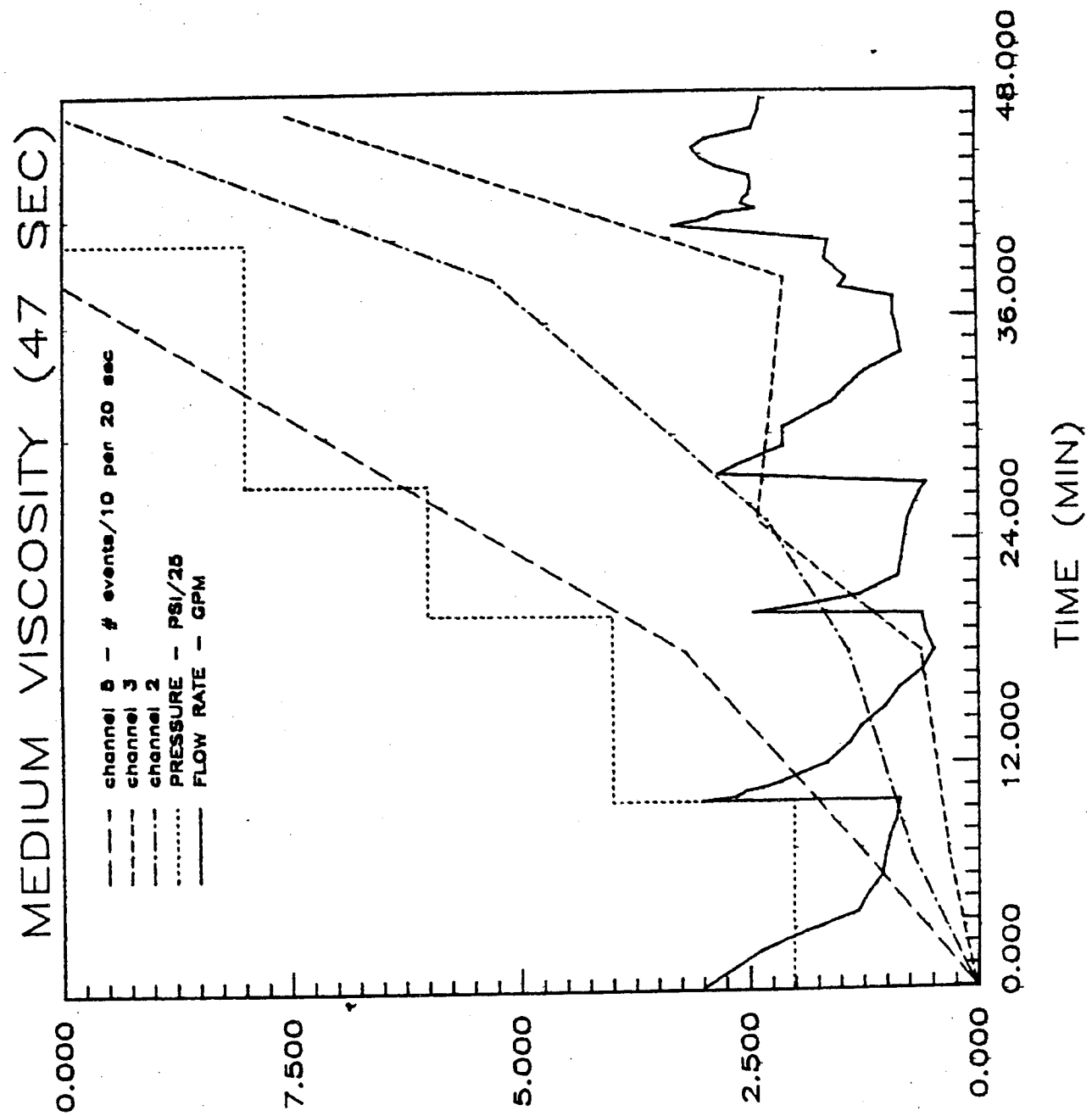
MEDIUM VISCOSITY (47 SEC)
channel 5 - # events/10 per 20 sec
channel 3
channel 2
PRESSURE - PSI/25
FLOW RATE - GPM
10.000
7.500
5.000
2.500
0.000
0.000
12.000
24.000
36.000
48.000
TIME (MIN)

FIGURE 8

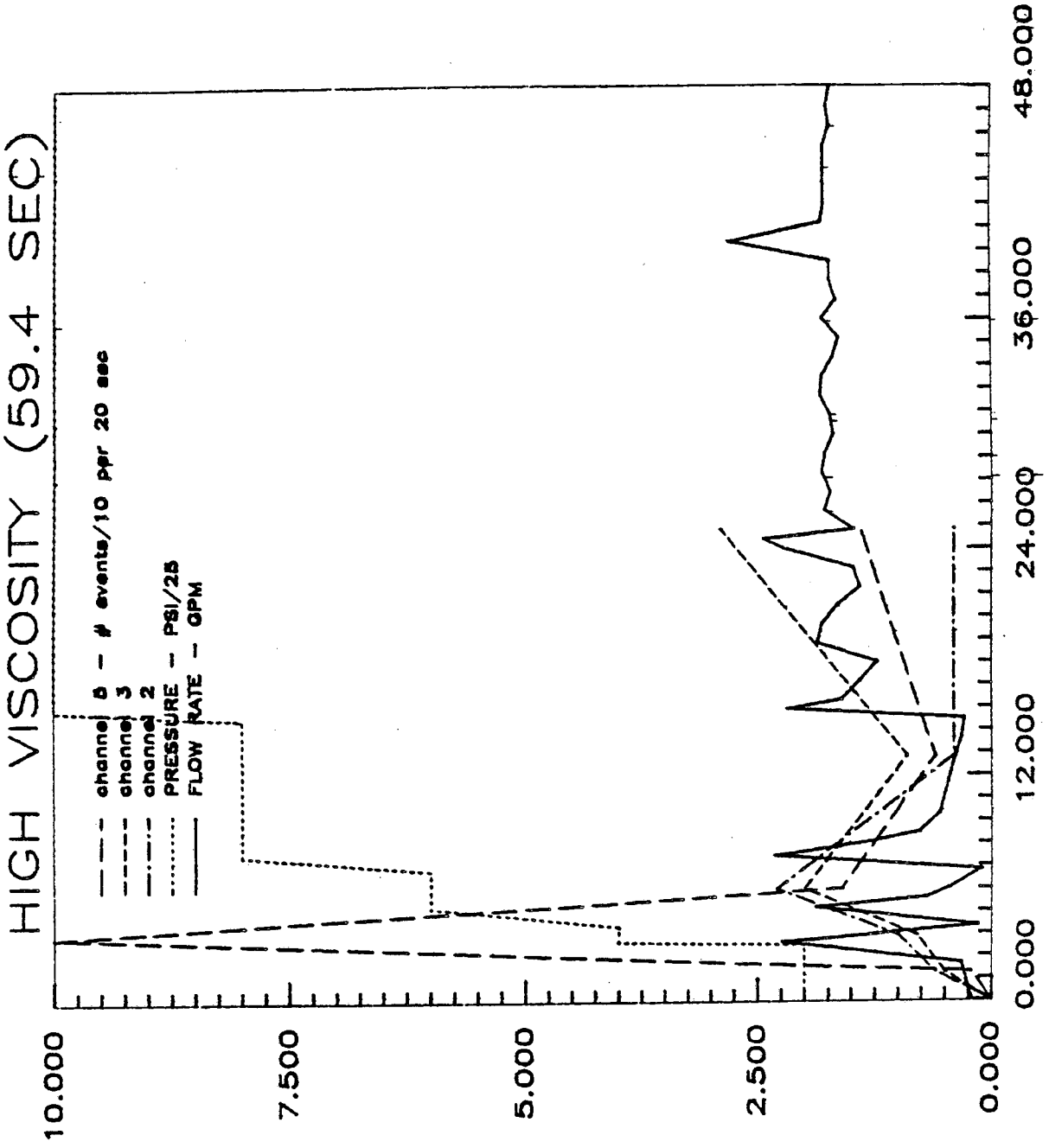
HIGH VISCOSITY (59.4 SEC)
channel 5 - # events/10 per 20 sec
channel 3
channel 2
PRESSURE - PSI/25
FLOW RATE - GPM
10.000
7.500
5.000
2.500
0.000
0.000
12.000
24.000
36.000
48.000
TIME (MIN)

FIGURE 9

Grout Injection Experiment
McNary Dam, Umatilla, Oregon

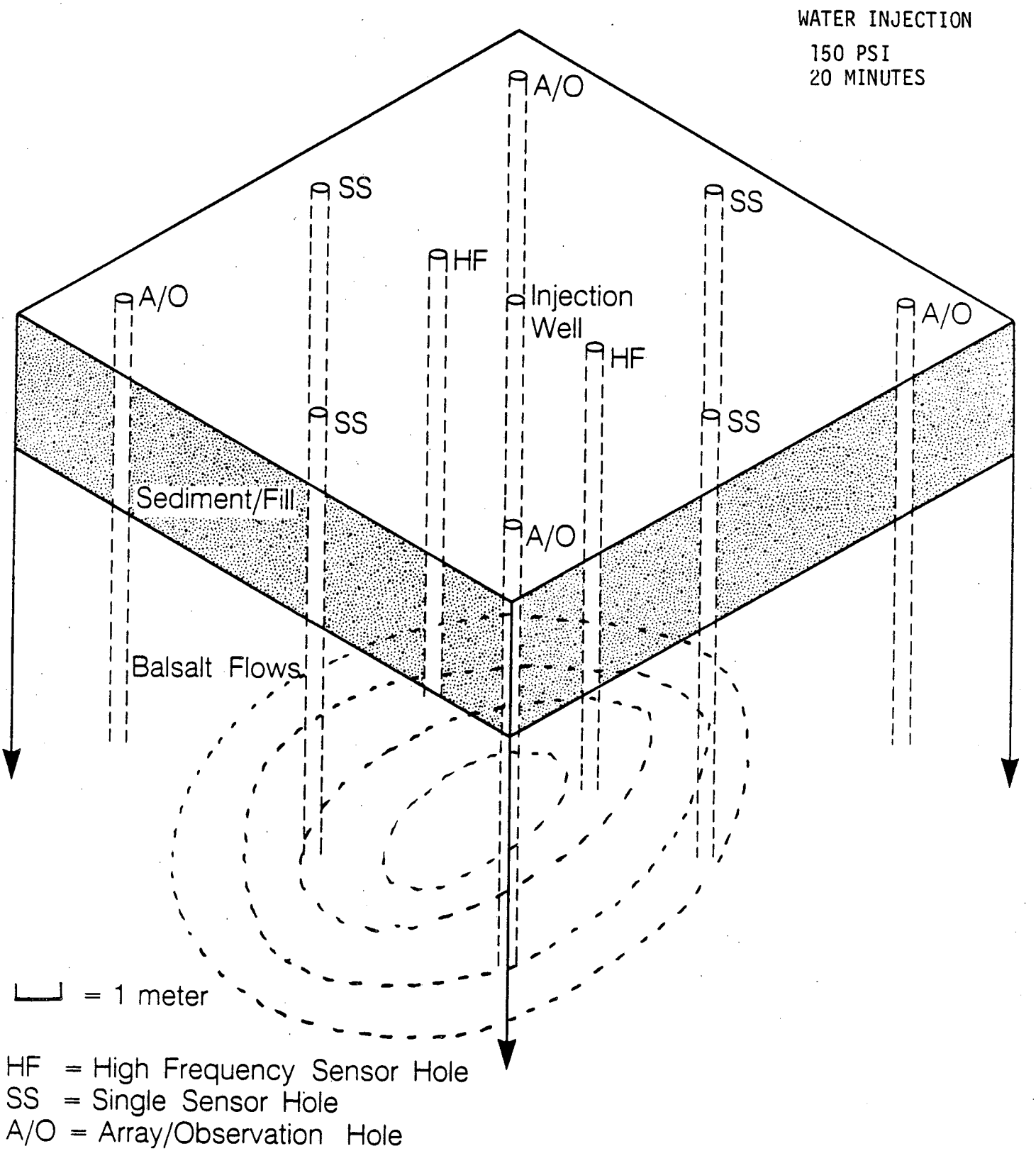

FIGURE 10

XBL 868-10957

Grout Injection Experiment
McNary Dam, Umatilla, Oregon

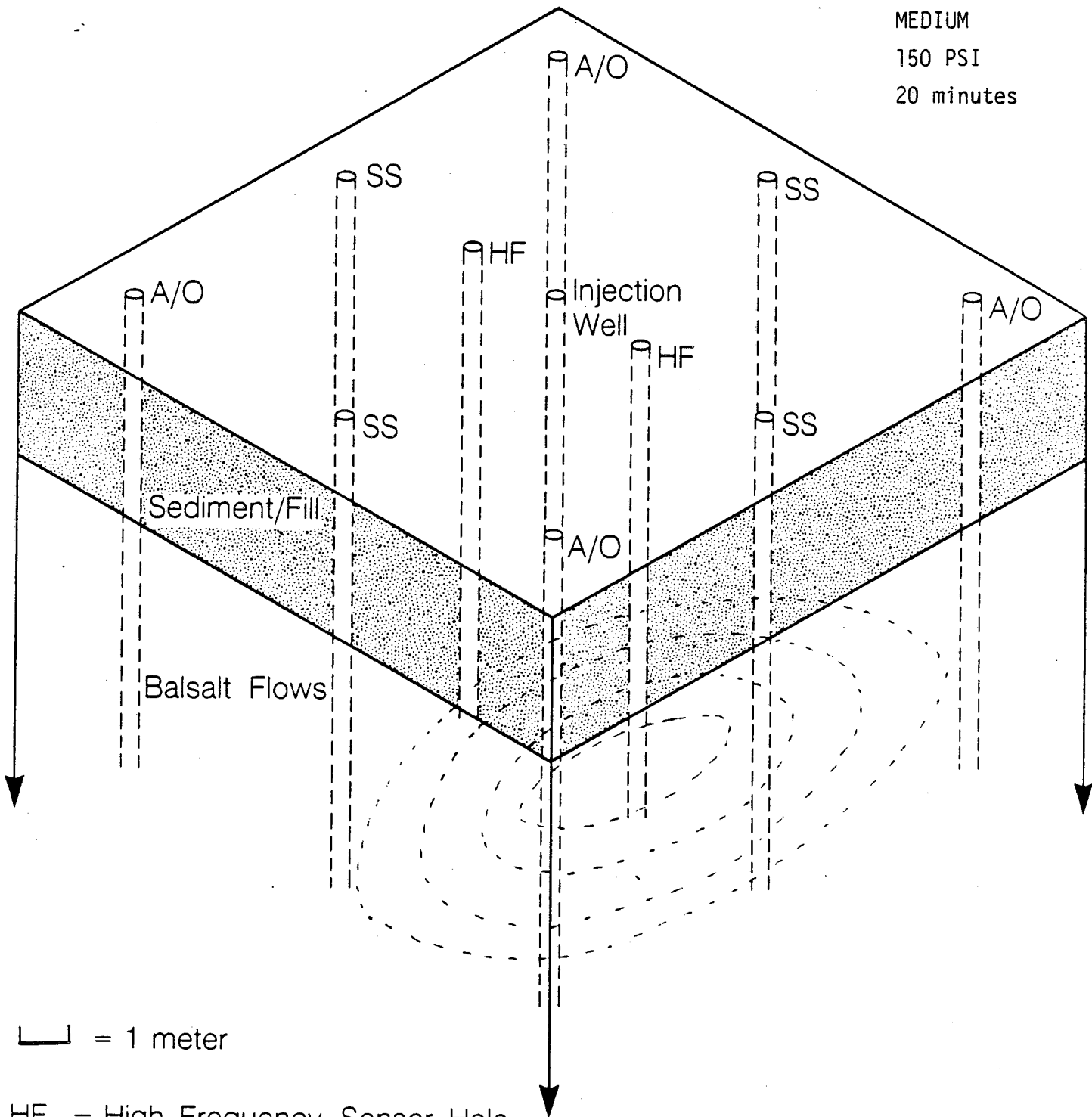

XBL 868-10957

FIGURE 11

LAWRENCE BERKELEY LABORATORY
TECHNICAL INFORMATION DEPARTMENT
UNIVERSITY OF CALIFORNIA
BERKELEY, CALIFORNIA 94720